

A Low-Noise Thrust Stand for Microthrusters with 25nN Resolution

Claude R. Phipps¹, James R. Luke^{1,2}, Wesley Helgeson²
and Richard Johnson²

¹*Photonic Associates LLC, 200A Ojo de la Vaca Road, Santa Fe, New Mexico USA 87508*

Phone/Fax: 1-505-466-3877, Email: crhipps@aol.com

²*NMT/IERA, 901 University Blvd, Albuquerque, NM, USA 87106*

Abstract. Accurate measurement of thrust from microthrusters is a significant technical challenge. We report significantly improved performance from our microthruster thrust stand which has now demonstrated 25nN thrust resolution and can carry a fully operational microthruster and power supply with up to 15kg total mass. Thrust capacity is 500 μ N with 0.5% accuracy and minimum response with 25% accuracy is 100nN. Because it is a critically-damped torsion balance with tens-of-seconds response time, thrust readout noise is essentially absent for frequencies above 0.1Hz. Other reported measurement techniques require careful leveling of the apparatus, or have higher readout noise, lower sensitivity and greater sensitivity to ambient mechanical vibrations. A key ingredient for the performance of our system design is an optical readout that responds only to rotation of the torsion bar, but not to ambient vibration. This feature eliminates sensitivity to footsteps, nearby vacuum pumps, etc. We will describe the design, calibration and testing of the optical readout.

Distribution A: Approved for public release; distribution unlimited

NOMENCLATURE

<p>C_m = laser momentum coupling coefficient = $F/\langle P \rangle$</p> <p>CPU = central processing unit</p> <p>CW = “continuous wave”, continuous laser output rather than pulsed</p> <p>$DPSS$ = diode-pumped, solid state</p> <p>d = diameter of torsion fiber</p> <p>E = short for “10[^]”</p> <p>f = laser pulse repetition frequency</p> <p>F = thrust</p> <p>G = torsion modulus of pendulum fiber</p> <p>GAP = glycidyl azide polymer</p> <p>g_o = acceleration of gravity at Earth’s surface</p> <p>I = laser intensity on target</p> <p>I_{sp} = specific impulse = v_E/g_o</p> <p>J = polar moment of inertia of torsion fiber</p> <p>L = length of slit focus on target</p> <p>$LISA$ = laser interferometer space antenna</p> <p>$ms\mu LPT$ = ms-pulse micro laser plasma thruster</p> <p>M = optical magnification ratio</p>	<p>MIB = minimum impulse bit</p> <p>m = magnetic dipole moment</p> <p>N_1 = number of turns, small calibration coil</p> <p>N_2 = number of turns, large calibration coil</p> <p>$ns\mu LPT$ = ns-pulse micro laser plasma thruster</p> <p>$\langle P \rangle$ = average incident laser optical power</p> <p>Q^* = specific ablation energy = $W/\Delta m$</p> <p>R = range from target to optics (cm)</p> <p>T = torque</p> <p>v_E = exhaust velocity = $C_m Q^*$</p> <p>W = total laser energy incident on target</p> <p>w = width of slit focus on target</p> <p>Δm = total ablated mass</p> <p>η_{AB} = ablation efficiency = $C_m I_{sp} g_o / 2 = C_m I_{sp} / 0.204$</p> <p>$\eta_E$ = laser optical power out/electrical power in</p> <p>μ_o = permeability of free space</p> <p>θ = angle of rotation of torsion bar</p> <p>τ = laser pulse duration</p>
---	--

INTRODUCTION

A recent project required measuring thrust with sub-100nN-level precision. Simulations showed that, in the laser fluence regime of interest for tests driven by a microchip laser [100-300 kJ/m²], C_m was expected to be in the range 10 - 100 μ N/W. With $P = 106$ mW delivered through the target illumination train to the target by our Concepts Research, Inc. model CRLB-0001-1064 “microchip” laser used for some of the target interaction tests, thrust as small as 1.1 μ N needed to be measured with 2% accuracy, meaning that we ideally needed 25nN measurement precision. The lower end of the range of interest would be achieved by attenuating the laser, resulting in thrusts as small as 300nN, measurements for which good precision was even more important.

This, in turn, forced us to redesign the thrust stand we have been using [1] for much higher resolution readout while retaining its 15kg carrying capacity.

Smaller forces are, of course, easily measured in a device that doesn’t have to carry this much mass. Our small torsion pendulum [2], intended for target sample qualification, can measure forces as small as 4nN, but its carrying capacity is just 10 grams.

At first, we tried to obtain increased resolution by creating a Mach-Zehnder interferometer incorporating a corner-cube retroreflector attached to the end of the torsion bar inside the test chamber as one mirror, with the other three optics situated on the optical table outside the vacuum test chamber. After equalizing paths and

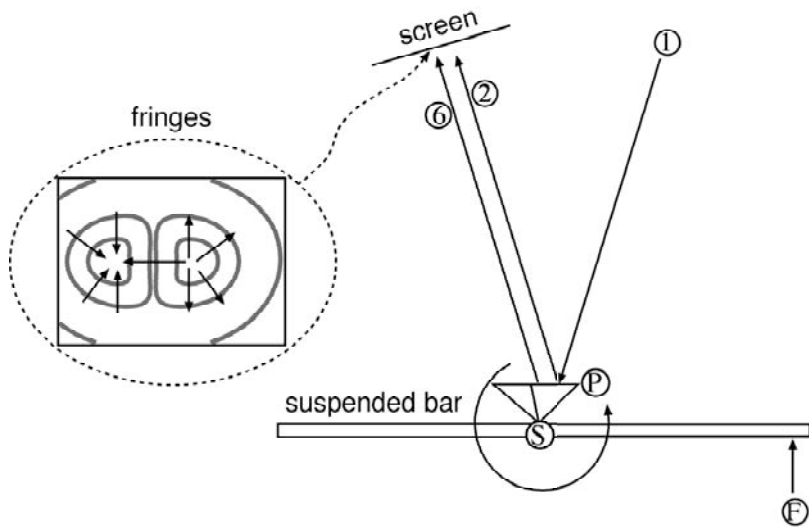


Figure 1A. Schematic of torsion bar rotation interferometer, viewed from above. “P” is the retroreflector.

determining that the coherence length of our probe laser matched the expected change of optical path length during thrust measurements, we found two disadvantages with this technique. First, the $2\mu\text{rad}$ rotation resolution (corresponding to 3nN) was an order of magnitude smaller than the $20\mu\text{rad}$ which we required to resolve 25nN . Second, any vibration, especially

the 140 Hz input from the spinning target holder which was part of the ns-pulse $\mu\text{thruster}$ mounted on the torsion bar, totally erased the interference fringes we were observing.

We settled on an optical readout design that gave just the required resolution and was sensitive only to rotation, not translation. The result could well tolerate the spinning target disk mounted directly on the thrust stand, and environmental inputs such as laboratory foot traffic and floor-mounted rotating forepumps.

INTERFEROMETER DESIGN

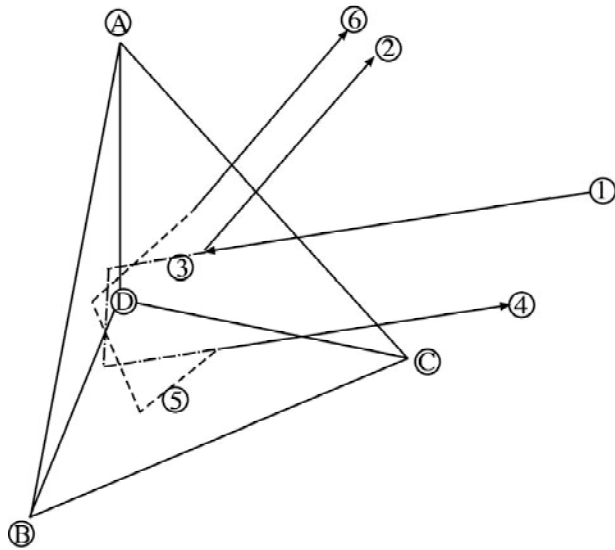


Figure 1B. Illustrating the origin of beams (2) and (6) in Figure 1A.

To measure rotation of the torsion bar, we developed a new type of optical interferometer not previously reported in the literature [Figures 1A and 1B]. The retroreflector “P” has 2.54cm diameter aperture. Beam (1) in Figure 1A is a 5mW , 532-nm near-diffraction-limited CW beam expanded to 15mm collimated diameter using a beam expansion telescope. The torsion bar is suspended from a $254\text{-}\mu\text{m}$ diameter steel fiber. In Figure 1A, this attachment point is indicated as “S”, and the microthruster applies thrust at point F. A solid glass “corner cube” retroreflector prism “P” is mounted to the bar

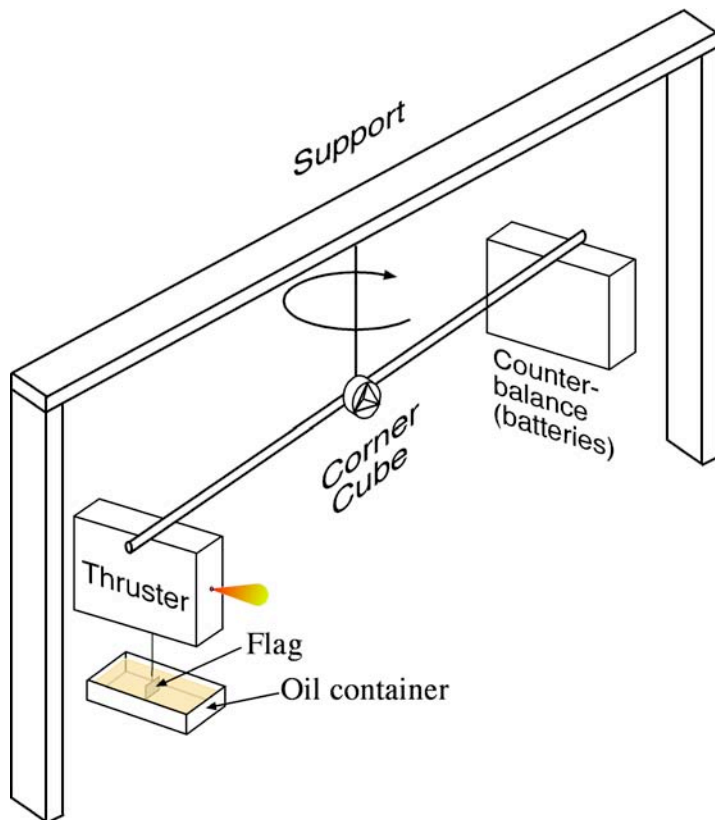


Figure 2. Thrust stand setup. Power supply is on board the thrust measurement bar with the thruster, and command and data transfer uses an IR data link, so that the only mechanical connection with the outside world is the 254- μm diameter steel fiber supporting the bar. An interferometer based on a solid glass retroreflecting “corner cube” (described below) is the key to resolving rotation of the bar. Critical damping is provided by a flag immersed in diffusion pump oil.

prism is a solid glass object with vertices (A), (B), (C) and (D). The angles made by the edges at (D) are all 90 degrees, hence “corner cube”. Beam (1) strikes the front face ABC producing the reflected beam (2). It also passes through the uncoated prism face and, after two internal reflections, produces external beam (4) which is exactly antiparallel to beam (1). Generation of beam (4) is the normal application of a corner cube. However, beam (4) also reflects internally off face ABC, producing beam (5) which, after two internal reflections, produces external beam (6). Beam (6) is precisely parallel to beam (2), independent of the cube orientation to beam (1). The phase difference between the beams (2) and (6) varies as the prism is rotated with respect to beam (1) due to small, angle-dependent differences between the total path length of beams (2) and (6), producing the interference fringes which are the basis of the rotation measurement.

close to the center. Beam (1) strikes the corner cube and produces two reflected beams (2) and (6). The initial angle between beam (1) and beams (2) and (6) is adjusted to about 30mrad to optimize sensor performance. These interfere on a screen, producing the fringes shown in the inset. As rotation occurs, these fringes move radially outward (as illustrated by the arrows in the inset) or inward, depending on the direction of rotation of the bar. Counting the passage of the fringes, which can be done visually or using an electronic data logger, gives rotation.

The origin of beam (6), which results from two internal roundtrips through the prism, is illustrated in greater detail in Figure 1B. The corner cube

Figure 2 shows how this interferometer was incorporated into the test stand. The setup is identical to the thrust stand reported in [1] except for a) 40-cm rather than 10-cm torsion fiber length, b) the critical damping attachment and c) the interferometer element in the center of the support bar. The latter replaces the simple mirror used as a rotation readout in [1]. The entire setup mounts inside our vacuum test chamber.

Thrust F is given by

$$F = k\theta/R \tag{1}$$

where $k = GJ/L = \pi d^4 G / (32L)$. (2)

In our case, $k = 194 \text{ pN}\cdot\text{m}/\mu\text{rad}$ and $R = 0.155\text{m}$, so that $k/R = 1.25\text{nN}/\text{mrad}$. This means that 25nN precision corresponds to $20\mu\text{rad}$ bar rotation, which the rotation sensor interferometer must resolve.

COMPARISON TO OTHER ONE-PIECE INTERFEROMETERS

The retroreflector function resembles that of a simple planar etalon in some ways, but there are important differences in detail.

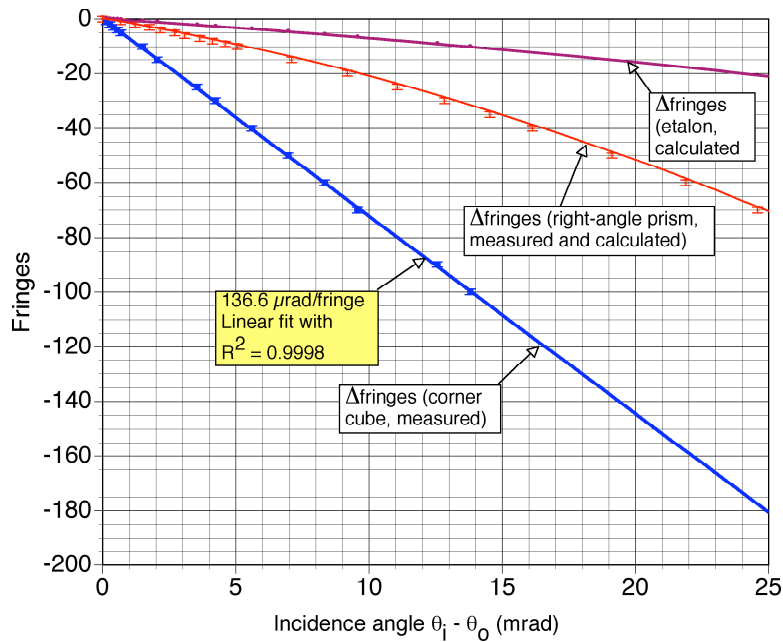


Figure 3. Calibration curve for the corner cube compared to that calculated for an etalon of similar depth. A zero-fringe incidence angle of 30mrad is assumed for the etalon calculation. At this angle, the prism is ten times more effective than the etalon, and its response is linear at any incidence angle. Both the etalon and the right-angle prism are distinctly nonlinear.

First, because of the complex internal optical path, the prism is ten or more times as effective in creating optical path difference compared to an etalon with the same thickness as the prism depth.

Second, unlike an etalon, for which the phase shift is quadratic with incidence angle, the fringe shift in the prism is absolutely linear with rotation [Figure 3].

Quadratic phase shift leads to calibration constants and sensitivity which must be specified

Table 1. Test Stand Performance	
Prism diameter (cm)	2.54
Prism depth (cm)	0.90
Sensor response ($\mu\text{rad}/\text{fringe}$)	136.6
Force response (nN/ μrad)	1.25
Force response (nN/fringe)	171
Maximum thrust measurable [using interferometer] (μN)	100
Minimum thrust measurable with 25% precision [using interferometer] (nN)	100
Minimum angular resolution (μrad)	20
Corresponding precision (nN)	25
Maximum thrust measurable [using conventional mirror] (μN)	500
Minimum thrust measurable with 25% precision [using conventional mirror] (μN)	8
Precision with conventional mirror (μN)	2
Load capacity (kg)	15

separately with each new incidence angle.

Linear phase shift is a unique advantage of the prism, making absolute calibration possible.

Also plotted in Figure 3 is the calculated response of a planar etalon having the same thickness as the prism depth and equal refractive index.

Table 1 summarizes the device performance, and compares it to the performance obtained with a mirror rather than an interferometer located at the torsion bar center of rotation, which we used in [1]. Although only 2.5 cm in diameter, the prism has the same angular resolution (20 μrad) as the diffraction-limited beam-width of a 6.5-cm

diameter optic at its 532nm operating wavelength.

To appreciate how small the resolved forces are, consider the C_{mhv} of reflected light (no ablation), 6.7nN/W. With our balance, the pressure of a 4W collimated light beam should just be measurable. Also, the gravitational attraction of the experimenter standing 50cm from the microthruster should also be barely observable, although well beneath the noise level of the device. We did not do either of these measurements, due to lack of a good collimated 4W laser source in the first instance, and to inadequate sensitivity for a believable measurement in the second.

INTERFEROMETER CALIBRATION AND TEST

Torsion balance calibration was based on the magnetic torque between a large, fixed Helmholtz coil and a small, centered rotatable Helmholtz coil attached to the torsion bar. This is a primary calibration. The procedure is described in more detail in [1].

For the two coils (a_2 and a_1 are the radii of the large and small coils, respectively), the torque T is

$$T = mB = \frac{\mu_0 \pi a_1^2}{2 a_2} i_1 i_2 N_1 N_2 \quad \text{N-m} \quad (3)$$

We used $N_1=20$ and $N_2=300$. We measured the pendulum rotation vs. combinations of i_1 and i_2 with $a_2=0.219\text{m} \gg a_1=0.039\text{m}$ to determine, for the case where the torsion fiber was 10cm long, $T = 774 \mu\text{N}\cdot\text{m}/\text{rad} \pm 10\%$. We then extended the torsion fiber length to 40cm for these measurements, and calculated

$$T = 194 \mu\text{N}\cdot\text{m}/\text{rad} \pm 10\% . \quad (4)$$

With $R = 15.5 \text{ cm}$, the thrust response of the device becomes

$$F = 1.25 \text{ nN}/\mu\text{rad} , \quad (5)$$

as indicated in Table 1. The sensor calibration is shown in Figure 4, where its response is compared to that of an etalon of the same depth, both at 30mrad initial incidence angle.

THRUST MEASUREMENTS

Figure 4 shows an example of data taken on our ns-pulse microthruster with the test stand we have described.

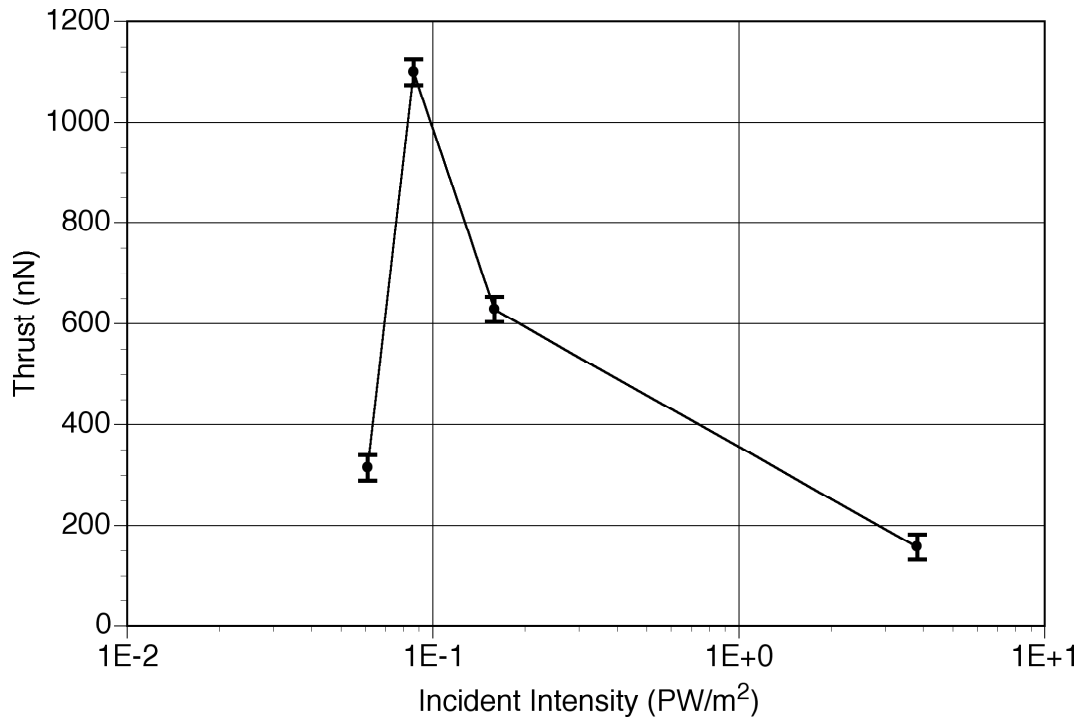


Figure 4. Thrust vs. intensity for ns-pulse microthruster obtained with the 25nN torsion balance. These data were obtained with a Quantel repetitively-pulsed laser delivering an attenuated average optical power $\langle P \rangle = 10 - 12\text{mW}$ at $f = 10\text{Hz}$, 4.5ns pulse duration to a gold target.

CONCLUSIONS

We built and tested a torsion balance thrust stand with 25nN precision, capacity from 100nN to 500 μ N and mass capacity 15kg. The thrust stand's optical rotation readout is a new type of interferometer, 2.5 cm in diameter, which responds only to rotation, not translation and has 20 μ rad rotational resolution.

REFERENCES

1. C. R. Phipps, J. R. Luke, T. Lippert, M. Hauer and A. Wokaun, "Micropropulsion using a laser ablation jet", *J. Prop. & Power*, **20** no.6, 1000-1011 (2004)
2. Phipps, C. R. and Luke, J. R., "Diode Laser-driven Microthrusters: A new departure for micropropulsion," *AIAA Journal* **40** no. 2 2002, pp. 310-318